

Computational study of Au₄ cluster on a carbon nanotube with and without defects using QM/MM methodology

Diana Barraza-Jimenez · D. H. Galvan ·
Alvaro Posada-Amarillas ·
Manuel Alberto Flores-Hidalgo ·
Daniel Glossman-Mitnik · Miguel Jose-Yacaman

Received: 29 February 2012 / Accepted: 30 May 2012 / Published online: 21 June 2012
© Springer-Verlag 2012

Abstract We use ONIOM (QM/MM) methodology to carry out geometry calculations in a 4-atom nanocluster supported by an (8, 8) armchair carbon nanotube with and without defects employing LSDA/SDD for the QM system and UFF for MM. In two particular cases, defects were added in the carbon nanotube wall. These defects are a double oxygenated vacancy (Vac₂O₂) and a double vacancy but without oxygen which creates two pentagons and an octagon. Our results show how geometries using QM/MM and energies calculations carried out with QM, change on both the gold nanocluster and the carbon nanotube. In addition, an application of ONIOM methodology in a comparative study to predict behavior of structures as hybrid materials based in carbon

nanotubes combined with gold nanoclusters is shown. In this work we examine geometry changes on both the gold nanocluster and the carbon nanotube. A comparison is made with the binding energy resulting values as well as with the orbital energies such as the frontier orbitals HOMO and LUMO.

Keywords Gold cluster · Oxygenated vacancies · QM/MM · SDD · Vacancies CNT

Introduction

Even though gold is one of the more inert metals in nature due to its low capability to react, this element has interesting properties in catalysis and applications in chemical sensors when found in nanometric sizes [1, 2]. For that reason there are an increasing amount of groups working in theoretical calculations with the aim of understanding the electronic structure of gold nanoclusters assembled in a wide diversity of forms, combinations and sizes that can reach 5 nm [3–9]. Alternatively, carbon nanotubes are among the more studied materials in the research field due to its interesting mechanical and electrical properties identified since their discovery [10] and highly regarded in different areas such as chemistry, physics, materials and biology. Hybrid materials formed by carbon nanotubes and gold put together features that enabled their implementation in devices used in relevant areas such as medicine. An example of these applications are carbon nanotubes covered with a gold layer as image detection, an agent in the detection of cancerogeneous cells in the linfatic system [11]. Other applications that stand out in latest years are related to employing gold nanoparticles supported by carbon nanotubes which at the end improve gold electric conductivity as well as optical capability and also a capability to exert attraction on biomolecules [12, 13].

D. Barraza-Jimenez (✉)
Centro de Investigacion en Alimentacion y Desarrollo
A.C. Unidad Delicias,
Av. 4^{ta} Sur 3820, Fracc. Vencedores del Desierto. Cd,
Delicias, Chih, Mexico 33089
e-mail: dbarraza@ciad.mx

D. H. Galvan
Centro de Nanociencias y Nanotecnologia,
Universidad Nacional Autonoma de Mexico,
Carretera Tijuana-Ensenada Km 107,
Ensenada, Baja California, Mexico 22800

A. Posada-Amarillas
Departamento de Investigacion en Fisica, Universidad de Sonora,
Apdo. Postal 5-088, 83190 Hermosillo, Sonora, Mexico

M. A. Flores-Hidalgo · D. Glossman-Mitnik
Centro de Investigacion en Materiales Avanzados, S.C.,
M. de Cervantes 120, Complejo Industrial Chihuahua,
Chihuahua, Chih, Mexico 31109

M. Jose-Yacaman
Department of Physics and Astronomy,
University of Texas at San Antonio,
San Antonio, TX 78249, USA

Gold nanoparticles or small gold clusters are allocated in the carbon nanotube (CNT) surface with the intention of studying interactions between both materials, which should be as stable as possible. There are different ways in which it can be possible the nanoparticles or cluster adhesion to the CNT surface. CNT functionalization allows physicochemical features modification which would enable to extend applications if the CNT is combined with other materials, one of those materials is gold. There are different functionalization methods available, based in the organic functionals incorporation for CNTs. Such incorporation provides strong covalent and non-covalent bonds, solubility in solvents or CNT surface immobility [14]. Theoretical-experimental studies in CNTs, where oxygen plasma was used, were developed to calculate oxygen-gold interaction over the CNT surface [15]. Physics methods, in which surface defects benefit gold nanoparticles (NP's) over the CNT, give the advantage of not breaking sp^2 hybridization. Besides, it has been corroborated that in reality most of the CNTs do possess those kind of defects and, it is precisely over these defects where the gold NP or cluster anchors over the CNT [1].

To this date, theoretical studies developed on calculations related to CNTs with gold NP's or clusters were carried out employing periodic systems using density functional theory [1, 15–18]. Calculations made on palladium nanoclusters over the CNT surface were developed employing ONIOM [19, 20]. ONIOM (QM/MM), which stand for quantum mechanics and molecular mechanics, respectively) methodology is applicable to big systems with the objective of reducing computational cost [21, 22]. In this work we present a study on an (8, 8) armchair carbon nanotube where a gold nanocluster shaped like a rhombus is placed over the CNT surface using the ONIOM methodology to carry out an analysis about the interactions between the two systems. Our study was carried out in three different conditions. The first one consisting of a carbon nanotube in its pure form, the second one is formed by a CNT containing oxygenated vacancies and the third one formed by a CNT with wall defects which give origin to an octagon and two pentagons sideways. So far as we know a study about ONIOM methodology analyzing results of geometry parameters, orbital and binding energies applied to study a carbon nanotube in its pure form or one containing defects such as oxygenated vacancies or wall defects, all of them used to support the gold cluster, has not been done.

Computational details

Calculations were carried out using the series of programs Gaussian09 [23]. A 4-atom gold cluster was optimized employing a local spin functional approximation (LSDA) [24]. LSDA functional is considered a good option for

works in the solid state, but it is not the best option for molecular studies, however, tested in small molecules excellent results were obtained [25].

The selected nanotube is an (8,8) armchair carbon nanotube with 1 nm diameter, 1.36 nm length formed by 224 atoms of which 192 are carbon atoms and 32 are hydrogen atoms saturating the nanotube extremes to avoid the dangling bonds. The nanotube was optimized using the ONIOM method with (LSDA/D95:UFF). It is known LSDA has a trend to overestimate molecular binding energy [26], in our case we employed only as comparative reference method.

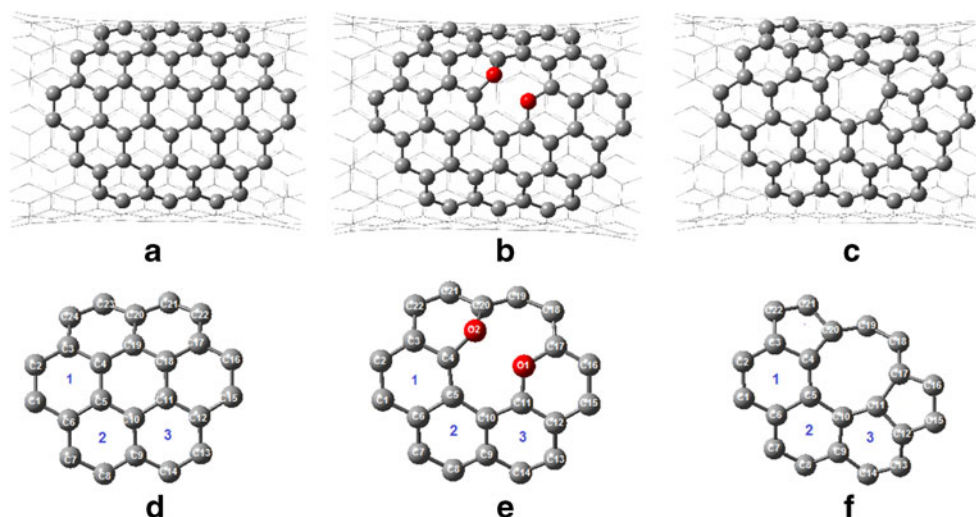
We used D95 basis set [27] for the high layer, formed as a circumcoronene, which consists of a coronene surrounded by benzene rings meanwhile the universal force field [28, 29] was employed for the rest of the nanotube atoms using two layers.

The nanotube was optimized in three different forms. In the first one, a nanotube without defects was optimized, in the second case two vacancies were created where the two subtracted carbon atoms were replaced by oxygen giving form to oxygenated vacancies (Vac_2O_2). In the third case, wall defects were introduced consisting of a modification in the wall by introducing two vacancies, and then, a free relaxation of the nanotube obtaining a new wall restructuration forming an octagon and two pentagons located next to the octagon sides was induced. When defects are incorporated, these defects are capable of acting like nucleation centers in the carbon nanotubes, allowing a better adsorption of particles or clusters [1].

In the three structures, once the carbon nanotube were optimized, a 4-atom gold cluster was placed. In Fig. 1, in the upper side, the three different optimized structures for the CNT can be observed and in the bottom side the basic structure with its coronene restructuration once optimized using QM can be observed.

Over the optimized nanotube in its different presentations, a 4-atom gold nanocluster was placed, which had its geometry previously optimized. After placing the gold cluster, we optimized the CNT+Au_4, employing again an ONIOM (LSDA/D95:UFF) two layer system. In this case, both the circumcoronene portion of the nanotube as well as the gold nanocluster (LSDA/SDD) were optimized together using the highest theoretical level available for QM. The rest of the nanotube atoms were optimized with a universal force field (UFF). A basis set SDD [30] was used as a first approximation. A Stuttgart/Dresden effective core potential basis set; (SDD) was employed showing optimum results working with transition metals including Au [5]. This methodology has shown good results on molecular structures of platinum (II) antitumor drugs, with the local spin density approximation (LSDA) functional [31]. In Fig. 2 one can observe CNT + Au_4 structures after the optimization. After the optimization, we carried out calculations to obtain the energy, but using the QM methodology for the whole system.

Fig. 1 CNT geometry optimization. (a) CNT in pure form, (b) CNT with Vac₂O₂, (c) CNT with wall defects, (d) Central coronene over a pure form CNT, (e) Modified coronene with Vac₂O₂ over the CNT, (f) Structure obtained by modification of the coronene placed over the CNT by incorporation of vacancies. Hexagons numbered from 1 to 3 without oxygenated vacancies or wall defects



Results and discussion

Parameters of geometry

Geometric parameters related to bond length are reported in Table 1 and Table 2. Bond length parameters used for comparative analysis were those related to the coronene portion of the nanotube which consists of seven benzene rings when speaking of the CNT in its pure form. Rings have been labeled according to Fig. 1, for its evaluation among the different interaction forms (this is CNT in its pure form, with oxygenated vacancy and wall defect). Table 1 shows bond lengths. For the gold cluster it can be observed that the bond length presenting the longer modification with a growing trend is the

one closer to the carbon nanotube surface and it is longer for the CNT in its pure form. Such an increment in the bond length indicates stabilization loss in the Au nanocluster, values presented in Table 3.

According to the data reported in the literature, bond length between atoms corresponding to a 5-atom gold nanocluster is 2.64 Å and 2.77 Å [18]. In our results a 4-atom gold nanocluster has bond length of 2.653 Å and 2.610 Å. Bond angle between atoms 1, 2, 3 was 58.9°, which agrees with reported data. The reported theoretical average distance between carbon atom and gold is 2.29 Å. Our calculations resulted in a bond length of 2.254 Å for this same bond. This same range of values corresponding to bond length C-Au has been reported by other groups with a value between 2.2 Å and 2.3 Å and the

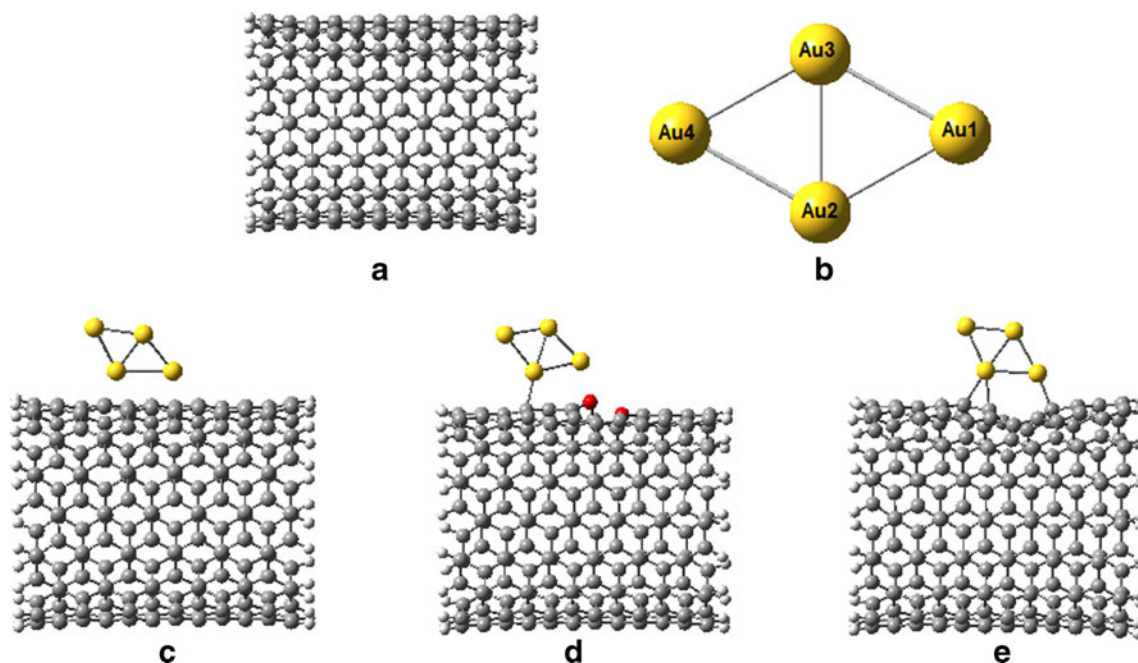


Fig. 2 CNT + Au₄ geometry optimization. (a) Isolated carbon nanotube without defects, (b) Isolated 4-atom gold cluster, (c) Pristine CNT + Au₄, (d) CNT + Au₄ with Vac₂O₂, (e) CNT + Au₄ with wall defects generated by double vacancy in the carbon nanotube

Table 1 Distances between gold nanocluster and CNT. Bond length in (Å)

Parameter	Au_4	CNT + Au_4	CNT Vac ₂ O ₂ + Au_4	CNT Def. + Au_4
Au(1)-Au(2)	2.653	3.000	2.792	2.821
Au(1)-Au(3)	2.653	2.559	2.566	2.601
Au(2)-Au(3)	2.610	2.639	2.637	2.620
Au(2)-Au(4)	2.653	2.617	2.629	2.631
Au(3)-Au(4)	2.653	2.671	2.665	2.665
Au(1)-C(10)		2.269		
Au(2)-C(6)		2.239		
Au(2)-C(2)			2.213	
Au(1)-O(2)			2.344	
Au(1)-C(17)				2.143
Au(2)-C(4)				2.182
Au(2)-C(3)				2.215
C(4)-O(2)			1.437	
C(11)-O(1)			1.350	
C(17)-O(1)			1.358	
C(20)-O(2)			1.417	

preferential location for that bond is found between two carbon atoms [18].

According to the data reported in the literature, bond length between atoms corresponding to a five atom gold nanocluster is 2.64 Å and 2.77 Å [18]. In our results a size four atom gold nanocluster had bond length of 2.65 Å and 2.61 Å. Bond angle between atoms 1, 2, 3 was 58.9°, which is in agreement with reported data. Average distance between carbon atom and gold is 2.29 Å. Our calculations resulted in a bond length of 2.26 Å for this same bond. This same range of values corresponding to bond length C-Au has been reported by other groups with a value between 2.2 Å and 2.3 Å and the preferential location for that bond is found between two carbon atoms [18].

In Table 2 we show geometric parameters of carbon hexagons unaffected neither by the incorporation of oxygenated vacancies nor by wall defects. One can observe that hexagon 2 shows the longer average bond length for both systems CNT + Au₄ as well as CNT Vac₂O₂ + Au₄. Incorporation of Au₄ nanocluster in the carbon nanotube with wall defect formed by octagon and pentagons affected more bond length in hexagon 1. In addition, one can observe in Fig. 2 that the binding preferred location for CNT + Au₄ with defect octagon-pentagon is the octagon.

According to experimental data, plasma oxygen over the CNT surface binds in the form C-O-C resulting in a decrement in the removal of oxygen species that would bind, weakly because of the Au atom, into the CNT surface with a binding energy of 5.0 eV [15]. This result is supported by our calculations as shown in Table 3.

Table 2 Bond length C-C (Å) for hexagons without defects forming part of the circumcoronene

Pristine	CNT		Oxyg. Vac.		with defect	
	CNT	CNT+ Au_4	CNT	CNT+ Au_4	CNT	CNT+ Au_4
Hexag. 1						
C(1)-C(2)	1.422	1.442	1.415	1.437	1.414	1.401
C(2)-C(3)	1.421	1.414	1.405	1.437	1.398	1.424
C(3)-C(4)	1.428	1.434	1.419	1.441	1.445	1.489
C(4)-C(5)	1.422	1.404	1.419	1.405	1.414	1.457
C(5)-C(6)	1.428	1.448	1.466	1.478	1.474	1.449
C(1)-C(6)	1.421	1.452	1.428	1.421	1.433	1.445
Average	1.424	1.432	1.425	1.436	1.430	1.444
Hexag. 2						
C(5)-C(6)	1.428	1.448	1.466	1.478	1.474	1.449
C(6)-C(7)	1.421	1.437	1.428	1.427	1.428	1.431
C(7)-C(8)	1.421	1.420	1.426	1.425	1.418	1.413
C(8)-C(9)	1.420	1.421	1.417	1.417	1.417	1.416
C(9)-C(10)	1.428	1.447	1.441	1.441	1.458	1.458
C(5)-C(10)	1.422	1.435	1.469	1.469	1.472	1.452
Average	1.423	1.435	1.441	1.443	1.444	1.437
Hexag. 3						
C(9)-C(10)	1.428	1.447	1.441	1.441	1.458	1.458
C(10)-C(11)	1.422	1.435	1.397	1.397	1.419	1.427
C(11)-C(12)	1.427	1.427	1.408	1.409	1.436	1.422
C(12)-C(13)	1.421	1.420	1.410	1.407	1.390	1.393
C(13)-C(14)	1.421	1.424	1.415	1.415	1.395	1.395
C(9)-C(14)	1.420	1.414	1.431	1.428	1.422	1.422
Average	1.423	1.428	1.417	1.416	1.420	1.420

Energy results

Results obtained in our study were compared with data reported by other groups. For the 4-atom gold cluster, the calculated HOMO-LUMO energy was 1.01 eV [6], while for the rhombus-type gold cluster we obtained 1.007 eV.

Table 3 Frontier orbitals energy, H-L energy, BE and stabilization energy for all three CNT structures in its isolated form and with incorporation of an Au₄ cluster

Structure	HOMO (eV)	LUMO (eV)	H-L (eV)	BE (eV)	S (eV)
CNT pristine	-4.758	-4.407	0.351	-	-
CNT Vac ₂ O ₂	-4.806	-4.379	0.426	-	-
CNT with defect	-4.856	-4.405	0.452	-	-
CNT + Au ₄	-4.894	-4.531	0.363	2.577	-0.644
CNT Vac ₂ O ₂ + Au ₄	-4.929	-4.508	0.421	5.005	-1.251
CNT Def + Au ₄	-4.949	-4.435	0.514	3.807	-0.952

For the selected carbon nanotube size which was considered as a small cluster, our results obtained for energy had variation from the reported data but only slightly in the range of hundredths of eV. This result can be perceived for the HOMO frontier orbital, for the CNT without Au₄ nanocluster.

In Table 3 one can observe that HOMO energy for the nanotube without defect presented the higher value. On the other hand, the lower HOMO energy value was obtained at the carbon nanotube with octagon-pentagon wall defect. LUMO energy level for the CNT with and without defect resulted in similar values but CNT Vac₂O₂ showed the higher LUMO level. From this, it is observed that the oxygenated vacancies presence increases the LUMO level which hinders the metallic character observed in this kind of nanotube. When obtained the difference between frontier orbitals for CNT structures in their pristine form as well as after gold was incorporated, CNT Vac₂O₂ presented the bigger difference between LUMO energy levels and this same structure was the only one that presented a decrement in its HOMO-LUMO gap energy with respect to the energy value calculated for the isolated form.

The narrower HOMO-LUMO gap energy was observed for the nanotube in its isolated form without any defect, the calculated value approaches the value reported in the literature for a (6,6) finite length carbon nanotube [32]. For the carbon nanotube containing the gold cluster the higher value was observed at the CNT + Au₄ with defect. The CNT with the incorporation of the gold cluster without defect had a 3.42 % increment in its HOMO-LUMO gap energy with respect to the same nanotube in its isolated presentation. CNT + Au₄ with defect had an 18.85 % increase in its HOMO-LUMO gap energy. In contrast CNT + Au₄ with oxygenated vacancies HOMO-LUMO gap energy decreased by 6.21 %. Binding energy as a measure of stabilization in CNT + Au₄ was calculated using the next equation:

$$BE = (E_{CNT} + E_{Au_4}) - E_{CNT+Au_4} \tag{1}$$

where BE is the binding energy for the carbon nanotube-gold cluster system. The first term between parenthesis corresponds to the carbon nanotube energy for each one of its different structures with and without defect. The second term is the energy for the rhombus-type gold cluster. The third term,

Table 4 First ten orbitals, including frontier orbitals with its electronic contributions by atom, considering atoms forming the coronene structure for studied CNT

Orb.	CNT pristine	CNT + Au ₄	CNT Vac ₂ O ₂	CNT Vac ₂ O ₂ + Au ₄	CNT with defect	CNT with defect + Au ₄
H-9		Au(3)-d=0.34 Au(4)-d=0.33 Au(1)-d=0.16		C(4)-p=0.04	C(15)-p=0.04	C(11)-p=0.03
H-8		Au(3)-d=0.21 Au(4)-d=0.18 Au(1)-d=0.11		Au(1)-d=0.14	C(16)-p=0.04	Au(1)-d=0.13
H-7			O(2)-p=0.02	Au(1)-d=0.06	C(12)-p=0.04	Au(3)-d=0.09
H-6		Au(3)-d=0.04		Au(3)-d=0.07		
H-5				Au(1)-d=0.06		C(11)-p=0.03
H-4						
H-3				C(4)-p=0.02		
H-2			C(4)-p=0.02	Au(1)-s=0.05		
H-1		Au(4)-s=0.28 Au(1)-s=0.16 Au(3)-p=0.16	O(1)-p=0.06	Au(4)-s=0.30 Au(3)-p=0.13 Au(1)-s=0.13	C(4)-p=0.05	Au(4)-s=0.17
H			C(22)-p=0.02		C(22)-p=0.04	C(22)-p=0.04
L			C(22)-p=0.02		C(19)-p=0.03	Au(4)-s=0.07
L + 1		Au(2)-s=0.05	C(10)-p=0.03	C(4)-p=0.07	C(17)-p=0.06	
L + 2		Au(3)-s=0.04				
L + 3						Au(2)-s=0.02
L + 4			C(11)-p=0.04			
L + 5		C(7)-p=0.03				
L + 6						
L + 7		Au(3)-p=0.07	C(15)-p=0.06	Au(3)-p=0.05		
L + 8		Au(1)-s=0.04	C(16)-p=0.06	C(17)-p=0.03		Au(3)-p=0.08
L + 9	C(1)-p=0.02	C(1)-p=0.04	C(12)-p=0.03			

which is being subtracted, corresponds to the energy of the whole system including both the CNT and the gold cluster.

Additionally and to compare, we calculated the stabilization using the next equation:

$$S = \frac{(E_{\text{CNT+Au}_4} - E_{\text{CNT}} - E_{\text{Au}_4})}{\text{Number of gold atoms}} \quad (2)$$

The system formed by the carbon nanotube containing oxygenated vacancies in combination with the gold cluster had the higher binding energy with 5.0 eV, followed by the carbon nanotube with octagon-pentagon defect and the last one was the carbon nanotube without defects. The calculated absolute value for the last one corresponding to S was 0.644 eV which is similar to 0.66 eV reported in the literature for a pristine graphene layer [15]. Literature reports a binding energy of 4.0 eV for a (5,5) carbon nanotube with double vacancy [1]. In our study, a (8,8) CNT employing ONIOM methodology resulted in 3.807 eV for the structure containing wall defect.

Also, we observed in Table 4 that electronic contributions for an isolated CNT in its pure form were absent. This result means an absence of the interactions needed to form covalent bonds. For CNT Vac₂O₂ we observed that all atoms located in the central hexagon had influence on the first ten orbitals but with low contribution. This supports the idea that CNT Vac₂O₂ is the more stable system. For the carbon nanotube with effect, the contributors were three carbon atoms, two of those, bonded to the gold nanocluster. Regarding the molecular system formed by the carbon nanotube and the gold cluster, we observed CNT + Au₄ had a significant electronic contribution in d orbitals at the HOMO levels from H-9 through H-6. This can be conferred to the non-bonding interaction between the gold nanocluster and the CNT. It was CNT Vac₂O₂ + Au₄ system the one containing the most occupied orbitals. Among those are the carbon atom bonded to the oxygen atoms but in small contributions going from 2 % through 7 %.

Au(4) is the atom containing the larger electronic contribution in all three cases. Relativistic effects appeared at HOMO-1 for all three structures formed by the carbon nanotube and the gold nanocluster. None of the three structures exhibited electronic contributions at gold atom d orbitals in the LUMO levels. Therefore, it is not possible to achieve an interaction where covalent bonds can exist, given that the larger electronic contributions are found farther from the nanotube center.

HOMO frontier orbital was occupied also with larger electronic contribution because of CNT + Au₄ with oxygenated vacancies.

Bonds formed between gold atoms in contact with the carbon nanotube are unstable according to our results shown at the molecular orbitals calculation.

Conclusions

QM/MM methodology allowed us to develop a comparative study with carbon nanotubes which were subject to strong structural changes when a rhombus-type gold nanocluster was anchored to the nanotube. The longest bond length change was observed at the nanocluster anchored to the CNT in its pristine form. This is an indication of the opposition to join if the CNT does not have a defect. Binding energy results were in agreement with the trend shown in the structural changes. Another outcome from our study is that the higher the binding energy, the smaller the change in the cluster bond length. Structure CNT Vac₂O₂ + Au₄ was the only one presenting a HOMO-LUMO decrease relative to the isolated CNT presentation (without gold cluster). For all three structures LUMO level decreased distinctly its energy with gold cluster incorporation. Relativistic effects were evident in LUMO orbitals for all three structures, being CNT with Vac₂O₂ the exception presenting p orbitals only, although weaker, and conferring higher stabilization to the structure.

Acknowledgments DBJ and APA thank Dr. Lauro Oliver Paz-Borbon from the Catalysis Research Center at Chalmers University of Technology for his technical support and valuable discussions. Also, authors thank Supercómputo UNAM (Universidad Nacional Autónoma de México) for computational resources used on theoretical calculations.

References

1. Yong-An L, Yan-Hong C, Xiao-Nian L, Xiang-Zhi S, Jian-Guo W MD (2010) The point-defect of carbon nanotubes anchoring Au nanoparticles. *Physica E* 42:1746–1750
2. Brodersen SH, Grønberg U, Hvolbæk B, Schiøtz J (2011) Understanding the catalytic activity of gold nanoparticles through multi-scale simulations. *J Catal* 284:34–41
3. Häkkinen H, Landman U (2000) Gold clusters (Au_N, 2 ≤ N ≤ 10) and their anions. *Phys Rev B* 62(4):2287–2290
4. Wang J, Wang G, Zhao J (2001) Density functional study of Au_n (n = 2–20) clusters: lowest-energy structures and electronic properties. *Phys Rev B* 66(3):1–6
5. Bulusu S, Zeng XC (2006) Structures and relative stability of neutral gold clusters: Au_n (n=15–19). *J Chem Phys* 125(154303):1–5
6. Koskinen P, Häkkinen H, Seifert G, Sanna S, Frauenheim Th, Moseler M (2006) Density-functional based tight-binding study of small gold clusters. *New J Phys* 8:1–11
7. Sankaran M, Viswanathan B (2006) A DFT study of the electronic property of gold nanoclusters (Au_x, x = 1–12 atoms). *Bul Catal Soc India* 5:26–32
8. Bulusu S, Li X, Wang LS, Zeng XCh (2007) Structural transitions from pyramidal to fused planar to tubular to core/shell compact in gold clusters: Au_n- (n=21–25). *J Phys Chem C* 111:4190–4198
9. Tian D, Zhao J (2008) Competition among fcc-Like, double-layered flat, tubular cage, and close-packed structural motifs for medium-sized Au_n (n=21–28) clusters. *J Phys Chem A* 112:3141–3144
10. Iijima S (1991) Helical microtubules of graphitic carbon. *Nature* 354:56–58
11. Kim JW, Galanzha EI, Shashkov EV, Moon HM, Zharov VP (2009) Golden carbon nanotubes as multimodal photoacoustic

- and photothermal high-contrast molecular agents. *Nat Nanotechnol* 4:688–694
12. Pannopard P, Khongpracha P, Probst M, Limtrakul J (2008) Structure and electronic properties of “DNA-gold-nanotube” systems: a quantum chemical analysis. *J Mol Graph Model* 26:1066–1075
 13. Jha N, Sundara R (2010) Development of Au nanoparticles dispersed carbon nanotube-based biosensor for the detection of paraxon. *Nanoscale* 2:806–810
 14. Jiang L, Gao L (2003) Modified carbon nanotubes: an effective way to selective attachment of gold nanoparticles. *Carbon* 41:2923–2929
 15. Suarez-Martinez I, Bittencourt C, Ke X, Felten A, Pireaux JJ, Ghijssens J, Drube W, van Tendeloo G, Ewels CP (2009) Probing the interaction between gold nanoparticles and oxygen functionalized carbon nanotubes. *Carbon* 47:1549–1554
 16. Da Silva AJR, Carrizo-Faria J, Da Silva EZ, Fazzio A (2003) Adsorption of gold atoms on carbon nanotubes. *Nanotech Technical Proceedings of the 2003 Nanotechnology Conference and Trade Show, Volume 3 Chapter 3: carbon. Nanostructures 165-168*, ISBN: 0-9728422-2-5
 17. Charlier JC, Arnaud L, Delgado M, Avilov IV, Demoisson F, Espinosa EH, Ewels CP, Felten A, Guillot J, Ionescu R, Leghrib R, Llobet E, Mansour A, Migeon HN, Pireaux JJ, Reniers F, Suarez-Martinez I, Watson GE, Zanolli Z (2009) Carbon nanotubes randomly decorated with gold clusters: from nano2hybrid atomic structures to gas sensing prototypes. *Nanotechnology* 20 (1-10):375501
 18. Deepak J, Pradeep T, Waghmare UV (2010) Interaction of small gold clusters with carbon nanotube bundles: formation of gold atomic chains. *J Phys Condens Matter* 22(125301):1–6
 19. Duca D, Ferrante F, La Manna G (2007) Theoretical study of palladium cluster structures on carbonaceous supports. *J Phys Chem C* 111:5402–5408
 20. Prasomsri T, Shi D, Resasco DE (2010) Anchoring Pd nanoclusters onto pristine and functionalized single-wall carbon nanotubes: a combined DFT and experimental study. *Chem Phys Lett* 497:103–107
 21. Svensson M, Humbel S, Froese RDJ, Matsubara T, Sieber S, Morokuma K (1996) ONIOM: A multi-layered integrated MO+MM method for geometry optimizations and single point energy predictions. A test for Diels-Alder reactions and Pt(P(t-Bu)₃)₂+H₂ oxidative addition. *J Phys Chem* 100:19357–63 (a)
 22. Dapprich S, Komáromi I, Byun KS, Morokuma K, Frisch MJ (1999) A new ONIOM implementation in Gaussian 98. 1. The calculation of energies, gradients and vibrational frequencies and electric field derivatives. *J Mol Struct (THEOCHEM)* 462:1–21
 23. Frisch MJ, Trucks GW, Schlegel HB, Scuseria GE, Robb MA, Cheeseman JR, Scalmani G, Barone V, Mennucci B, Petersson GA, Nakatsuji H, Caricato M, Li X, Hratchian HP, Izmaylov AF, Bloino J, Zheng G, Sonnenberg JL, Hada M, Ehara M, Toyota K, Fukuda R, Hasegawa J, Ishida M, Nakajima T, Honda Y, Kitao O, Nakai H, Vreven T, Montgomery JA Jr, Peralta JE, Ogliaro F, Bearpark M, Heyd JJ, Brothers E, Kudin KN, Staroverov VN, Kobayashi R, Normand J, Raghavachari K, Rendell A, Burant JC, Iyengar SS, Tomasi J, Cossi M, Rega N, Millam NJ, Klene M, Knox JE, Cross JB, Bakken V, Adamo C, Jaramillo J, Gomperts R, Stratmann RE, Yazyev O, Austin AJ, Cammi R, Pomelli C, Ochterski JW, Martin RL, Morokuma K, Zakrzewski VG, Voth GA, Salvador P, Dannenberg JJ, Dapprich S, Daniels AD, Farkas Ö, Foresman JB, Ortiz JV, Cioslowski J, Fox DJ (2009) *Gaussian 09, Revision A.1*. Gaussian Inc, Wallingford, CT
 24. Vosko SH, Wilk L, Nussair M (1980) Accurate spin-dependent electron liquid correlation energies for local spin density calculations: a critical analysis. *Can J Phys* 58:1200–1211
 25. Painter GS (1986) Density functional description of molecular bonding within the local spin density approximation. *J Phys Chem* 90(22):5530–5535
 26. Martin RL, Illas F (1997) Antiferromagnetic exchange interactions from hybrid density functional theory. *Phys Rev Lett* 79(8):1539–1542
 27. Dunning TH Jr, Hay PJ (1976) In: Schaefer HF III (ed) *Modern theoretical chemistry*, vol 3. Plenum, New York, pp 1–28
 28. Rappé AK, Casewit CJ, Colwell KS, Goddard WA III, Skiff WM (1992) UFF a full periodic-table force-field for molecular mechanics and molecular-dynamics simulations. *J Am Chem Soc* 114:10024–35. doi:10.1021/ja00051a040
 29. Rappé AK, Colwell KS, Casewit CJ (1993) Application of a universal force field to metal complexes. *Inorg Chem* 32(16):3438–3450
 30. Andrae D, Haeusserrmann U, Dolg M, Stoll H, Preuss H (1990) Energy-adjusted *ab initio* pseudopotentials for the 2nd and 3rd row transition-elements. *Theor Chem Acta* 77:123–41
 31. Gao H, Xia FY, Huang CJ, Lin K (2011) Density functional theory calculations on the molecular structures and vibration spectra of platinum(II) antitumor drugs. *Spectrochim Acta A* 78:1234–1239
 32. Rochefort A, Salahub DR, Avouris PJ (1999) Effects of finite length on the electronic structure of carbon nanotubes. *Phys Chem B* 103: 641–646